Microscopic Analysis of a Thermal Brownian Motor

C. Van den Broeck,[1] R. Kawai,[2] and P. Meurs[1]

[1]*Limburgs Universitair Centrum, B-3590 Diepenbeek, Belgium*
[2]*Department of Physics, University of Alabama at Birmingham, Birmingham, Alabama 35294, USA*

We study a genuine Brownian motor by hard disk molecular dynamics and calculate analytically its properties, including its drift speed and thermal conductivity, from microscopic theory.

It is (believed to be) impossible to systematically rectify thermal fluctuations in a system at equilibrium. Such a perpetuum mobile of the second kind, also referred to as a Maxwell demon [1], would violate the second law of thermodynamics and would, from the point of view of statistical mechanics, be in contradiction with the property of detailed balance. Yet, it may require quite subtle arguments to explain in detail on specific models why rectification fails. Apart from the academic and pedagogical interest of the question, the study of small scale systems is motivated by rapidly increasing capabilities in nanotechnology and by the huge interest in small scale biological systems. Furthermore, when operating under nonequilibrium conditions, as is the case in living organisms, the rectification of thermal fluctuations becomes possible. This mechanism, also referred to as a Brownian motor [2], could furnish the engine that drives and controls the activity on a small scale. In this Letter we propose a breakthrough in the theoretical and numerical study of a small scale thermal engine. Our starting point is the observation that one of the basic and most popular models, namely, the Smoluchowski-Feynman ratchet [2–4], is needlessly complicated and can be replaced by a simplified construction involving exclusively hard core interactions. Its properties, including speed, diffusion coefficient, and heat conductivity, can be measured very accurately by hard disk molecular dynamics and can be calculated exactly from microscopic theory.

In Fig. 1(a), we have schematically depicted the construction originally introduced by Smoluchowski [4] in his discussion of Maxwell demons and reintroduced with two compartments at different temperatures by Feynman [3]. One compartment contains a ratchet with a pawl and a spring, mimicking the rectifier device that is used in clockworks of all kinds. The macroscopic mode of operation of such an object generates the impression that only clockwise rotations can take place, suggesting that this construction can be used as a rectifier of the impulses generated by the impacts of the particles in the other compartment on the blades with which the ratchet is rigidly linked. As Feynman has argued, such a rectification is possible only when the temperature in both compartments is different. We now introduce a model which is

at the same time a simplification and a generalization of this construction. First, we can dispose of the pawl and the spring in the ratchet and consider any rigid but asymmetric object. An example with a cone-shaped object in one compartment and a flat "blade" or "sail" located in the other one is illustrated in Fig. 1(b). Second, we replace the single rotational degree of freedom with a single translational degree of freedom [Figs. 1(c) and 1(d)]. Third, we restrict ourselves to two-dimensional systems. Finally, the substrate particles in the various compartments are modeled by hard disks which undergo perfectly elastic collisions with each other while their center collides elastically with the edges of the motor [5].

We first report on the results obtained from molecular dynamics for two different realizations of our motor. The first one, referred to as arrow-bar or *AB*, is inspired by the
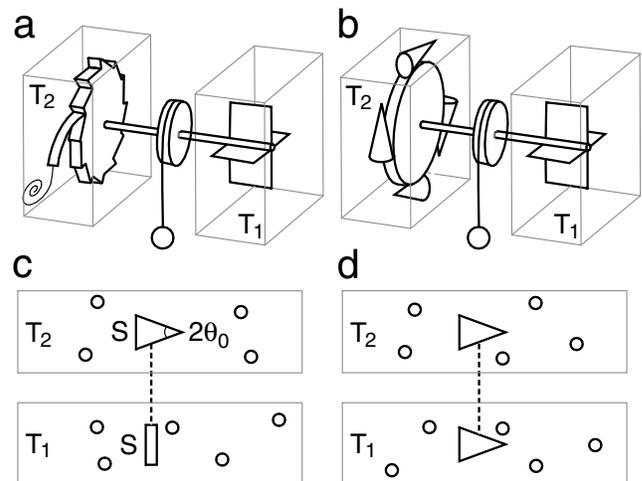
FIG. 1. (a) Schematic representation of the Smoluchowski-Feynman ratchet. (b) Similar construction without a pawl and a spring. (c) Two-dimensional analog referred to as the *AB* motor. The motor is constrained to move along the horizontal *x* direction (without rotation or vertical displacement). The host gas consists of hard disks whose centers collide elastically with the engine parts. The shape of the arrow is determined by the apex angle $2\theta_0$ and the vertical cross section *S*. Periodic boundary conditions are used in the computer simulations. (d) A symmetric construction referred to as the *AA* motor.

above discussion. It consists of one triangular-shaped arrow in the first compartment and a flat bar in the other [Fig. 1(c)]. The other motor, called arrow-arrow or AA, consists of an identical triangular-shaped arrow in both compartments [Fig. 1(d)]. Both units of the motor are constrained to move as a rigid whole along the horizontal x direction as a result of their collision with the hard disks in the two compartments. The initial state of the hard disk gases corresponds to uniform (number) densities ρ_1 and ρ_2 and Maxwellian speeds at temperatures T_1 and T_2, in compartments 1 and 2, respectively [6] ($k_B = 1$ by choice of units). The boundary conditions are periodic both left and right and top and bottom. Unless mentioned otherwise, the following parameter values are used: Each compartment is a 1200 by 300 rectangle and contains 800 hard disks (mass $m = 1$, diameter 1); i.e., particle densities $\rho_1 = \rho_2 = 0.00222$. Initial temperatures were set to $T_1 = 1.9$ and $T_2 = 0.1$. The motor has a mass $M = 20$, apex angle $2\theta_0 = \pi/18$, and vertical cross section $S = 1$. The averages are taken over 1000 runs.

When the temperatures are the same in both compartments, $T_1 = T_2$, no rectification takes place. In fact, Fig. 2 shows that the motor undergoes plain Brownian motion, with average zero speed, exponentially decaying velocity correlations, and linearly increasing mean square displacement. The corresponding friction and diffusion coefficient obey the Einstein relation. On the other hand, as soon as the temperatures are no longer equal, the motor spontaneously develops an average systematic drift along the x axis. The amplitude and direction of the speed depend in an intricate way on the parameters of the problem. In particular, the average speed increases with the temperature difference and the degree of asymmetry (decreasing θ_0) and decreases with increasing mass of the motor roughly as $1/M$ (see the lower panel in Fig. 3). Note furthermore that the observed average speed can be very large, i.e., comparable to the thermal speed $\sqrt{k_B T/M}$
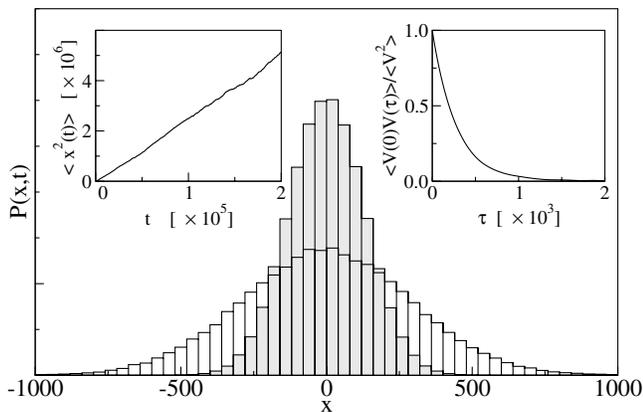
of the motor. The AA motor has a peculiar behavior, resulting from the fact that both units are identical. Whereas equilibrium is usually a point of flux reversal, the velocity now displays a parabolic curve as a function of $T_1 - T_2$ with a minimum equal to zero at the equilibrium state $T_1 = T_2$. It is clear from its symmetric construction that, at least when $\rho_1 = \rho_2$, an interchange of T_1 with T_2 cannot modify the speed so that the latter has to be an even function of $T_1 - T_2$, cf. Fig. 3.

We finally note that the observed systematic speed does not persist forever. Indeed, the motion of the motor along the x direction is a single degree of freedom that allows for (microscopic) energy transfers and hence thermal contact between the compartments, a fact that was overlooked by Feynman in his analysis and first pointed out in
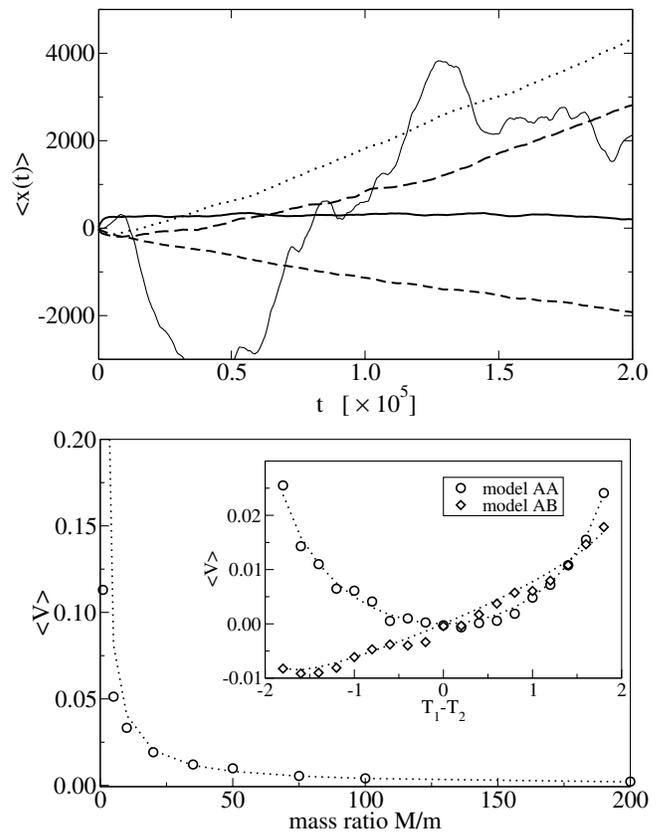
FIG. 3. Upper panel: position of the motor as a function of time. The thin solid curve shows a typical trajectory. All other curves represent the average $\langle x(t)\rangle$. The thick solid line is the equilibrium case ($T_1 = T_2 = 1$) for motor AB. The dotted and dashed curves correspond to the nonequilibrium situation for, respectively, motor AA and AB ($T_1 = 1.9$, $T_2 = 0.1$). The situation with switched temperatures for AB is the dashed curve with a negative velocity. Lower panel: average velocity of motor AB as a function of its mass M. Inset: average speed (average over 2000 runs) of motors AA and AB as a function of the initial temperature difference $T_1 - T_2$ ($T_1 + T_2 = 2$ fixed). The theoretical results (7) and (8) predict lower speeds than the simulations. However, when the magnitude is scaled, the theoretical curves (dotted lines) fit well with the simulations.

FIG. 2. Probability density $P(x, t)$ for the position x of motor AB at times $t = 1000$ (shaded) and $t = 4000$ (open). Left inset: mean square displacement versus time. Right inset: velocity correlation function.

[7,8]. As a result one observes that the temperatures in both compartments converge exponentially to a common final temperature with a concomitant reduction and eventual disappearance of the systematic motion as shown in Fig. 4. While this feature has already been documented in detail in other constructions [9], we have focused here on conditions in which this conductivity is small and the compartments sufficiently large so that one reaches a quasisteady state with a well defined and measurable average drift velocity.

To obtain analytic results from microscopic theory, which are asymptotically exact, we focus on the situation in which the compartments are infinitely large while the densities of the hard disk gases are extremely low (more precisely, the so-called high Knudsen number regime requires that the mean free path is much larger than the linear dimensions of the motor units). In this limit, each compartment, characterized by its particle density ρ_i and temperature T_i, acts as an ideal thermal reservoir. We furthermore assume that all the constituting units of the motor are closed and convex. Under these circumstances, the motor never undergoes recollisions and the assumption of molecular chaos becomes exact [10]. The probability density $P(V, t)$ for the speed $\vec{V} = (V, 0)$ of the motor thus obeys the following Boltzmann-Master equation:

$$\partial_t P(V, t) = \int dr [W(V - r, r)P(V - r, t) - W(V, r)P(V, t)]. \tag{1}$$

$W(V, r)$ is the transition probability per unit time for the motor to change speed from V to $V + r$ due to the collisions with the gas particles in various compartments. The explicit expression for $W(V, r)$ follows from elementary arguments familiar from kinetic theory of gases, taking into account the statistics of the perfectly elastic collisions of the motor, constrained to move along the
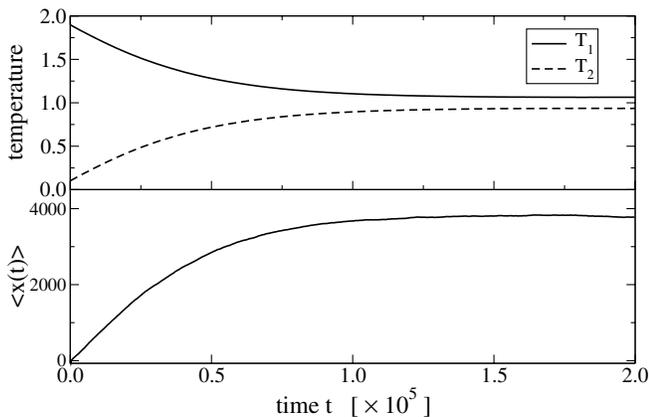
FIG. 4. Exponential decay of the temperatures to a final common value ($T_{\text{final}} = (T_1 + T_2)/2 = 1.$) in motor AB and concomitant disappearance of the average drift speed. To enlarge the conductivity, a small mass $M = 1$, a large vertical cross section $S = 10$, and a large apex angle $\theta_0 = \pi/9$ are used.

x direction, with the impinging particles:

$$W(V, r) = \sum_i \int_0^{2\pi} d\theta \int_{-\infty}^{\infty} dv_x \int_{-\infty}^{\infty} dv_y \rho_i \phi_i(v_x, v_y)$$
$$\times L_i F_i(\theta)(\vec{V} - \vec{v}) \cdot \vec{e}(\theta) H[(\vec{V} - \vec{v}) \cdot \vec{e}(\theta)]$$
$$\times \delta\left[r + \frac{m}{M} B(\theta)(V - v_x + v_y \cot\theta)\right]. \tag{2}$$

Here, the sum over i runs over all the different compartments, L_i is the total circumference of the ith unit of the motor, $B(\theta) = 2M\sin^2\theta/(M + m\sin^2\theta)$, $H[x]$ is the Heaviside function, and $\vec{e}(\theta) = (\sin\theta, -\cos\theta)$ is the unit vector normal to a surface at angle θ, $\theta \in [0, 2\pi]$, the angles being measured counterclockwise from the horizontal axis. $\phi_i(v_x, v_y) = m \exp[-m(v_x^2 + v_y^2)/2k_B T_i]/2\pi k_B T_i$ is the Maxwellian velocity distribution in compartment i. The shape of any closed convex unit of the motor is defined by the (normalized) probability density $F(\theta)$ such that $F(\theta)d\theta$ is the fraction of its outer surface that has an orientation between θ and $\theta + d\theta$. Note that $\langle \sin\theta \rangle = \langle \cos\theta \rangle = 0$, where the average is with respect to $F(\theta)$, a property resulting from the requirement that the object is closed.

The Boltzmann-Master equations (1) and (2) can now be solved by a perturbation expansion in $\sqrt{m/M}$, following a procedure similar to the one used in one-dimensional problems such as the Rayleigh piston [11] or the adiabatic piston [12]. The details are somewhat involved and will be given elsewhere [13]. To lowest order in the perturbation, the Master equation (1) reduces to a Fokker-Planck equation equivalent to the following linear Langevin equation:

$$M\dot{V} = -\sum_i \gamma_i V + \sum_i \sqrt{2\gamma_i k_B T_i}\, \eta_i \tag{3}$$

with η_i independent Gaussian white noises of unit strength and

$$\gamma_i = 4\rho_i L_i \sqrt{\frac{k_B T_i m}{2\pi}} \int_0^{2\pi} d\theta F_i(\theta)\sin^2\theta \tag{4}$$

the friction coefficient experienced by the motor due to its presence in compartment i. We conclude that at this order of the perturbation the contributions from the separate compartments add up and are each—taken separately—of the linear equilibrium form. In particular the motor has no (steady state) drift velocity, $\langle V \rangle = 0$. It does, however, conduct heat. In the case of the two compartments 1 and 2, the heat flow per unit time between them is, as anticipated in Ref. [7], given by a Fourier law: $\dot{Q}_{1 \to 2} = \kappa(T_1 - T_2)$ with conductivity $\kappa = k_B \gamma_1 \gamma_2/[M(\gamma_1 + \gamma_2)]$. One also concludes from (3) and (4) that the (steady state) velocity distribution of the

motor is Maxwellian, but at the effective temperature

$$T_{\text{eff}} = \sum_i \gamma_i T_i \Big/ \sum_i \gamma_i. \qquad (5)$$

At the next order of perturbation in $\sqrt{m/M}$, the corresponding Langevin equation becomes nonlinear in V while at the same time the Gaussian nature of the white noise is lost, a feature well known from the van Kampen $1/\Omega$ expansion [11]. The most relevant observation is the appearance, at the steady state, of a nonzero drift velocity:

$$\langle V \rangle = \sqrt{\frac{\pi k_B T_{\text{eff}}}{8M}} \sqrt{\frac{m}{M}} \frac{\sum_i \rho_i L_i \frac{T_i - T_{\text{eff}}}{T_{\text{eff}}} \int_0^{2\pi} d\theta F_i(\theta) \sin^3\theta}{\sum_i \rho_i L_i \sqrt{\frac{T_i}{T_{\text{eff}}}} \int_0^{2\pi} d\theta F_i(\theta) \sin^2(\theta)}. \qquad (6)$$

This speed is of the order of the thermal speed of the motor, times the expansion parameter $\sqrt{m/M}$, and further multiplied by a factor that depends on the details of the construction. Note that the Brownian motor ceases to function in the absence of a temperature difference ($T_i \equiv T_{\text{eff}}, \forall i$) and in the macroscopic limit $M \to \infty$ ($\langle V \rangle \sim 1/M$). Note also that the speed is scale independent, i.e., independent of the actual size of the motor units: $\langle V \rangle$ is invariant under the rescaling L_i to CL_i. To isolate more clearly the effect of the asymmetry of the motor on its speed, we focus on the case where the units have the same shape in all compartments, i.e., $F_i(\theta) = F(\theta)$. In this case T_{eff} is independent of $F(\theta)$ and the drift velocity is proportional to $\langle \sin^3\theta \rangle / \langle \sin^2\theta \rangle$, with the average defined with respect to $F(\theta)$. The latter ratio is in absolute value always smaller than 1, a value that can be reached for "strongly" asymmetric objects as shown below on a particular example.

We now turn to a comparison between theory and simulations. From the general result (6), one obtains the following expressions for the speed of the two motors that were studied:

$$\langle V \rangle_{AA} = \rho_1 \rho_2 (1 - \sin\theta_0)$$
$$\times \sqrt{\frac{m}{M}} \sqrt{\frac{\pi k_B}{8M}} \frac{(T_1 - T_2)(\sqrt{T_1} - \sqrt{T_2})}{[\rho_1 \sqrt{T_1} + \rho_2 \sqrt{T_2}]^2}, \qquad (7)$$

$$\langle V \rangle_{AB} = \rho_1 \rho_2 (1 - \sin^2\theta_0)$$
$$\times \sqrt{\frac{m}{M}} \sqrt{\frac{\pi k_B}{2M}} \frac{(T_1 - T_2)\sqrt{T_1}}{[2\rho_1 \sqrt{T_1} + \rho_2 \sqrt{T_2}(1 + \sin\theta_0)]^2}. \qquad (8)$$

In agreement with previous arguments, the AA motor, cf. (7), always moves in the same direction, namely, the direction of the arrow. Furthermore, it is an example where one can increase the asymmetry to generate a maximum drift speed. The limit $|\langle \sin^3\theta \rangle| = \langle \sin^2\theta \rangle$ is reached here when $\theta_0 \to 0$, which corresponds to an infi-

nitely elongated and sharp arrow in both compartments. Because of strong finite size effects (e.g., sound waves among others), the agreement between the theoretical results (7) and (8) and the computer simulations is only qualitative: the theory predicts speeds which are typically 20%–40% lower. However, Eqs. (7) and (8) can be fitted to the simulation results by appropriately rescaling the magnitude of the velocity (see Fig. 3), indicating that their dependencies on the parameters, M, T_1, and T_2, are in good agreement with the simulations.

The problem of the Maxwell demon has been haunting the imagination and theoretical efforts of physicists for more than a hundred years. It is thus reassuring that the analytical and numerical discussions of the microscopic model presented here are in agreement with the consensus that thermal fluctuations cannot be rectified in a system at equilibrium. In addition, our model provides an example of a genuine Brownian motor: the rectification of non-equilibrium thermal fluctuations appears outside the scope of linear irreversible thermodynamics, namely, at the level of nonlinear response, where the usual separation between systematic and noise terms, as made explicit in a linear Langevin equation, is no longer possible.

[1] H. S. Leff and A. F. Rex, *Maxwell's Demon* (Adam Hilger, Bristol, 1990).

[2] P. Reimann, Phys. Rep. **361**, 57 (2002).

[3] R. P. Feynman, R. B. Leighton, and M. Sands, *The Feynman Lectures on Physics I* (Addison-Wesley, Reading, MA, 1963), Chap. 46.

[4] M. v. Smoluchowski, Phys. Z. **13**, 1069 (1912).

[5] This trick avoids collisions of the disk's surfaces with the sharp corners of the motor; for more details; see C. Van den Broeck, R. Kawai, and P. Meurs, in *Noise in Complex Systems and Stochastic Dynamics*, edited by Lutz Schimansky-Geier, Derek Abbott, Alexander Neiman and Christian Van den Broeck, SPIE Proceedings Vol. 5114 (SPIE–International Society for Optical Engineering, Bellingham, WA, 2003), p. 1.

[6] Note that our system as a whole is finite and isolated so that strictly speaking the equilibrium state should refer to a microcanonical ensemble.

[7] J. M. R. Parrondo and P. Espagnol, Am. J. Phys. **64**, 1125 (1996).

[8] K. Sekimoto, J. Phys. Soc. Jpn. **66**, 1234 (1997).

[9] C. Van den Broeck, E. Kestemont, and M. Malek Mansour, Europhys. Lett. **56**, 771 (2001).

[10] J. R. Dorfman, H. Van Beijeren, and C. F. McClure, Arch. Mech. **28**, 333 (1976).

[11] N. G. van Kampen, *Stochastic Processes in Physics and Chemistry* (North-Holland, Amsterdam, 1981).

[12] Ch. Gruber and J. Piasecki, Physica (Amsterdam) **268A**, 412 (1999); E. Kestemont, C. Van den Broeck, and M. Malek Mansour, Europhys. Lett. **49**, 143 (2000).

[13] P. Meurs, C. Van den Broeck, and A. Garcia (to be published).